Suzaku wide-band observation of anomalous dips in Hercules X-1

Kazuhiro Nakazawa[1], Tsuyoshi Ueda[1], Teruaki Enoto[1],
Shin'ya Yamada[1] Motoko Suzuku[2] and Kazuo Makishima[1]

[1] The University of Tokyo, 7-3-1 Hongo, Bunkyo-ku, Tokyo 113-0033
[2] Japan Aerospace Exploration Agency, 2-1-1 Sengen, Tsukuba, Ibaraki 305-8505
E-mail(KN): nakazawa@phys.s.u-tokyo.ac.jp

ABSTRACT

Suzaku wide-band spectra of temporary dips of Hercules X-1 were analyzed. From the orbital phase, they are classified as anomalous dips. We successfully obtained the spectra from 0.3 to 60 keV with good statistics, and investigated the physical state of the absorbing materials. The HXD-PIN spectra in the 20–60 keV band allows us to estimate the total hydrogen absorption column as $\sim 20 \times 10^{22}$ cm^{-2}, in the deepest case, by attributing the dip mainly to the Thomson scattering. In the XIS soft X-ray spectra of the dips, signature of O VII edge was observed, suggesting ionized nature of the absorbing materials, with another evidence of partial covering. Time variability of the dips are typically explained by pile up of $\sim$200 s dips. Based on these observational results, we propose a model that the dips are made by a sum of two types of geometrically thin absorbers, with ionization parameter of $\sim$0.5 erg cm^{-1} and $\sim$15 erg cm^{-1} located around the edge of the accretion disk.

KEY WORDS: stars: puslars: individual: Her X-1 — X-rays: binaries — X-rays: dips

1. Introduction

Hercules X-1 (hereafter Her X-1) is a well-studied binary X-ray pulsar discovered by Uhuru (Tananbaum et al. 1972). Its X-ray variability is characterized by; the 1.24-s spinning, the 1.70-d orbital motion, the 35-d on/off cycle which is usually attributed to accretion disk precession, and sporadic intensity decrease for 1–10 ks, called a dip, presumably caused by obstracting materials passing through our line of sight (e.g. Giacconi et al. 1973). In this paper, we dicuss the dip phenomenon.

Since the discovery by Giacconi et al. (1973), the dip phenomenon has been studied extensively (Crosa and Boynton 1980, Ushimaru et al. 1989, Mihara et al. 1991, Reynolds and Parmar 1995, Leahy 1997, Stelzer et al. 1999, Shakura et al. 1999). According to these previous works, the dips are divided into two types; pre-eclipse dips and anomalous dips, occuring at pre-eclipse orbital phases and at random phases, respectively. From spectral studies of these data, the obscuring materials were suggested to be neutral by the EXOSAT observatory (Reynolds and Parmer 1995), or to be ionized by the Tenma satellite (Ushimaru et al. 1989). In these observations, however, the covered energy range were limited to within 2–17 keV and 2.5–35 keV, respectively.

The Suzaku observatory (Mitsuda et al. 2007) covers a wide band-path from 0.2 to 600 keV, and can provide improved knowledge on the dip phenomenon. In this paper, we investigate the ionization structure and possible locations of the obscuring materials causing dips in the Her X-1 system.

2. Observations

We observed Her X-1 three times with Suzaku since its launch, aiming at calibration of the timing and energy response (see Terada et al. 2008 and Enoto. et al. 2008, respectively). Among them, the second observation was held on 2006 March 29 UT 18:12 through March 30 15:22. The HXD was operated in the standard mode, while the XIS employed "1/8 window" option to improve the time resolution (to 1 s) and to avoid event pile up. Observation date are chosen to catch main-on phases of the 35-day cycle of Her X-1, and to avoid its eclipses. In this observation, we fortunately observed anomolous dips at a 1.7 day binary phase of $\Phi_{1.7} \sim$0.0–0.1, where $\Phi_{1.7} = 0$ is defined as the inferior conjunction of Her X-1.

Figure 1 shows three-band light curves of the 2nd observation; the soft and middle bands, which is 0.2–2.0 keV and 2.0–10.0 keV photons detected in the XIS-1 chip, respectively, and the hard band, which is 13–50 keV photons detected by the HXD-PIN. During the dips, the 0.2–2.0 keV count rate decreased to $\sim$ 10% of the normal rate, while that in 2–10 keV was halved. Furthermore, the dips are visible also in the HXD-PIN light curve.
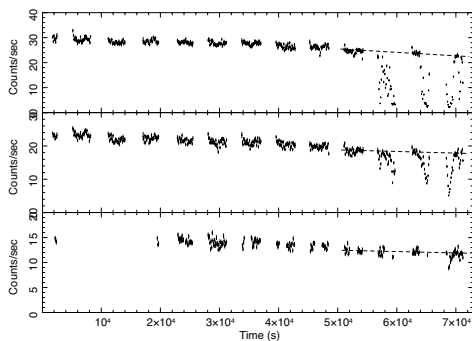
Fig. 1. Light curve of photons detected by XIS-1 in the 0.2–2.0 keV, the 2–10 keV, and by HXI-PIN in the 13-50 keV, from top to the bottom, respectively. Structures of dips are observed. Dashed lines are assumed long-term trend of the pulsar X-ray emission. Horizontal axis is the time since $19 : 29 : 46$, 29th March 2005 (UT).
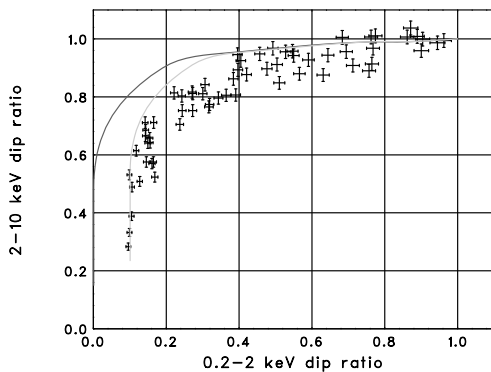

Fig. 2. Scatter plot of the depth of the dips in the soft (0.2–2.0 keV) and the middle (2–10 keV) bands. Model lines represent a typical case with cool absorber, and with 10% partial covering.

3. Timing Properties of the Dips

The variability of the energy dependence of the observed dips carry important information as to their origin. In figure 2, we show the scatter plot of "dip ratio", as the ratio of count rates in an energy range recorded during dips, to the assumed normal count rate corresponding to the non-dipping time. The non-dip count rate in a given energy range was calculated by fitting a linear function to the light curves over a period of $(5.0 - 7.2) \times 10^4$ s, manually excluding dip intervals. The fitted lines are shown as dashed lines in figure 1.

First of all, a clear trend is visible that the dip ratio of individual timing bins correlates to have a single curve, even though the plot is made up of many dips with different depth. Therefore, the source behavior during the dips is likely to be described by a single parameter, namely, the overall column density of the absorbing materials, even though the materials themselves may well have composite multi-zone structures. Below, we use these inferences for spectral analysis.

Table 1. Hydrogen column density of the three dip intervals.

	Shallow	Middle	Deep
$N_{\mathrm{H}}* \ (\times 10^{22} \ \mathrm{cm}^{-2})$	2.0–6.9	3.3–11	16–25

∗ Calculated from the Compton optical depth.

Secondly, the soft band dip depth saturates at 10%. This could be understood as an evidence of $\sim 10\%$ leak of direct emission, i.e. partial covering nature of the absorber.

Thirdly, these dips are not caused by a simple cold, i.e. neutral absorber. Prediction of dip ratio relation assuming a cold absorber is shown in figure 2 in two cases, with and without 10% of partial covering. The timing variability of dip ratio shows a bit flatter curve than these model, suggesting ionized nature of the absorber, i.e. "the warm absorber".

4. Spectral Analysis
4.1. A simple modeling

In this work, we utilized the spectra obtained from the XIS-1 and the HXD-PIN for simplicity, since the combination of these two devices provides us with the widest band coverage. The 0.3–50 keV combined spectra in the non-dip time region can be explained by a model employed in Oosterbroek et al. (1997), made of a powerlaw with a photon index of 0.8, a broad Fe-K line near 6.4 keV, a broad Fe-L line near 0.8 keV, and a ~ 0.1 keV blackbody. By adjusting normalizations of these components, this model reproduced the non-dip XIS spectrum to an accuracy of better than 1%.

Since the main focus of this work is only on absorption properties, however, we generated a ratio of the dip and non-dip spectra, and fitted the absorption model directly to the ratio spectra. As shown in the last section, the dip properties can be explained by one-parameter. Therefore, we defined three intervals in terms of the 2–10 keV dip ratio, 0.0–0.6, 0.6–0.8, and 0.8–1.1, to be called "deep dips", "middle dips", and "shallow dips", respectively. Then, we summed spectral data in each range to obtain spectra with higher statistics. Note that the long-term trend is removed in this analysis (see figure 1).

Thanks to the good sensitivity of HXD-PIN, the ratio spectra covers up to 50 keV, as shown in figure 4. Each ratio spectrum approaches a constant value toward higher energies, which is slightly lower than unity, even above 20 keV. By attributing this hard-band dip to Thomson scattering, we derived the hydrogen column density N_{H} as shown in table 1.

As already pointed out at the last section, a $\sim 10\%$ or larger fraction of direct component is evident. Thus, we tried a partial absorbing with cold material (hereafter

the "baseline model"). The $N_{\rm H}$ value is modeled to be consistent with the HXD-PIN derived one. The model requires much sharp cut-off in the soft-band spectra, and the fit was far from acceptable.
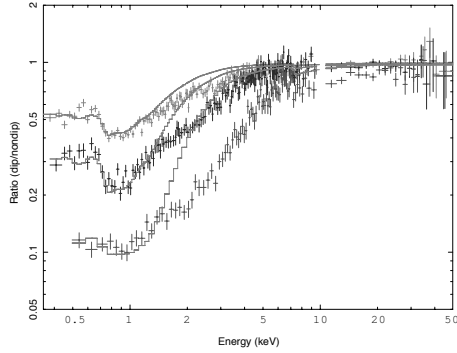

Fig. 3. The normalized dip spectra compared with the predictions of the "Baseline model" (orange).

In the soft band, the spectra are characterized by a dip-structure around 0.7–0.8 keV, and another structure around 1.7 keV apparent in the "deep dips" spectra. Those two structures cannot be easily generated via neutral absorber. In order to examine whether photo-ionized absorbers can explain these structures, we used a "warm absorber" model based on the software XSTAR ver. 2.1ln8[1] , parametrized by the ionization parameter $\xi = L/nr^2$. Here L is the central source luminosity, n is the absorber density, and r is the distance from the central source to the absorber.

4.2.   The tandem and parallel warm absorber models

Then we assumed that a part of the absorber is ionized, so that it can be explained by a multiplication of neutral and ionized absorber (hereafter "tandem model"). This model, however, cannot explain the structures at the 0.7 keV and 1.7 keV at the same time, and the fit is not acceptable. What is more, the ionization parameter ξ increases with the dip deepness, although the increasing $N_{\rm H}$ should cause decrease in ξ.

As another model, we tried a three component model made up of a partial dens warm absorber, another partial thin warm absorber, and the partial direct component (hereafter "parallel model"). The fitted parameters are shown in table 2, and the spectra is shown in figure 4. This model gives remarkably acceptable fit to all three spectra, event though the spectral shape is not complicated. Interestingly, ionization parameters ξ of the two components were kept nearly constant regardless of the dip depth. Thus, the "parallel model" suggests the existence of two typical types of absorbers.
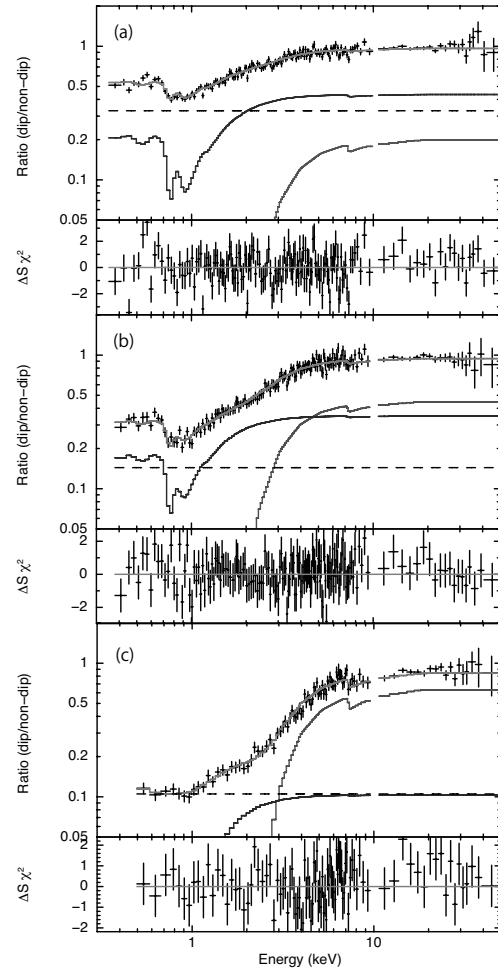
_____

[1]   see http://heasarc.gsfc.nasa.gov/docs/software/xstar/

Fig. 4. Dip ratio spectra fitted with two component partial absorption model, "the parallel model".

5.   Combined Analysis

Independent important information to reveal the nature of the absorber is hidden in the light-curve itself. Carefully looking into the light curve, we can identify a typical dip with a duration of ~ 200 sec. Even in the deepest dip, the ~ 200 sec structure is visible. This result suggests that there is a typical size of the blobs, and the depth of the dip may by connected with the piling-up effect of these blobs. If we assume that the blobs are located at the outer-edge of the accretion disk ($r = 2 \times 10^{11}$ cm) rotating in Keplerian motion, the 200 sec interval can be converted into geometrical width of $\sim 5 \times 10^9$ cm.

Ionization parameter ξ and column density $N_{\rm H}$ provides us with a typical line-of-sight thickness D of the absorber by assuming $L = 2.5 \times 10^{37}$ erg s^{-1} (the 1–50 keV luminosity by Enoto et al. 2008). The estimated value is $D = 1$ and 2×10^8 cm, for the dens and thin absorber components, respectively. If the absorber is located much nearer to the pulser, differences in W and D rapidly increases. Thus fact also suggests that they are

Table 2. Parameters of Parallel model

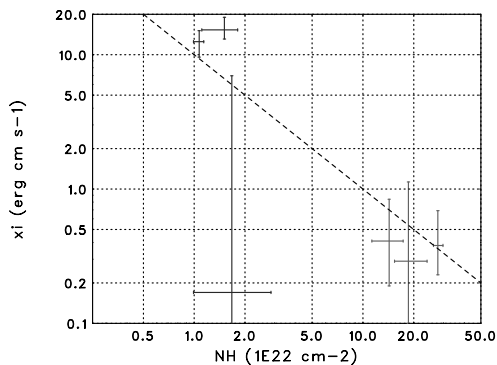| Dip	f	ξ^l (erg cm s^{-1})	f^l	$N_{\rm H}^l$ ($\times 10^{22}$ cm^{-2})	ξ^s (erg cm s^{-1})	$1-f-f^l$	$N_{\rm H}^s$ ($\times 10^{22}$ cm^{-2})	χ^2/dof
Shallow	0.33 +0.05 −0.05	0.29 +0.84 −0.19	0.23 +0.04 −0.03	18.6 +5.4 −3.2	15.3 +3.7 −2.2	0.44 +0.03 −0.04	1.51 +0.30 −0.40	210.5/152 = 1.38
Middle	0.14 +0.05 −0.05	0.41 +0.43 −0.22	0.50 +0.02 −0.04	14.3 +0.3 −3.0	12.5 +2.6 −2.9	0.35 +0.06 −0.03	1.07 +0.07 −0.08	144.9/155 = 0.93
Deep	0.11 +0.03 −0.03	0.38 +0.31 −0.15	0.79 +0.01 −0.02	27.8 +2.0 −1.6	0.17 +6.8 −0.16	0.11 +0.03 −0.02	1.67 +1.18 −0.68	89.9/93 = 0.97

Fig. 5. Ionization parameter as a function of $N_{\rm H}$ of thin (left crosses) and dens (right crosses) absorbers. Dashed line represents a correlation assuming the "disk outer-edge blob model"; absorbers are located $r = 2 \times 10^{11}$ cm, and the absorber thickness to the line-of-sight is $D = 1.6 \times 10^8$ cm (see text for detail.)

located at or near the disk outer-edge. Interestingly, the value of D is similar in two components, as shown in the $N_{\rm H}$ vs ξ plot in figure 5. In other words, both the two types of absorbers have similar line-of-sight thickness, regardless of the ionization state.

Since the width W of the blob is about 30-times larger than the typical thickness D of the absorber, and the ratio spectra can be successfully explained by the "parallel model", we propose a simple geometrical model of the absorbing material as follows. The absorber is located at the farthest point of the accretion disk from the companion star, HZ Her. They are made of tens of filaments with typical diameter of $D = 1.6 \times 10^8$ cm, with two-phase density, typically $n_{\rm dens} = 1.3 \times 10^{15}$ cm^{-3} and $n_{\rm thin} = 6 \times 10^{13}$ cm^{-3}. These filaments (or dots) form a blob with typical size of $W = 5 \times 10^9$ cm, crossing our line-of-sight to the central pulser. There are tens of blobs in total, forming the series of dip as seen in the spectra.

6. Summary and conclusions

Using Suzaku, we analyzed the 0.3–50 keV wide-band spectra of the anomalous dips of Her X-1. The dips are characterized by ~ 200 sec dip time scale, regardless of the depth of the dips. The 0.3–50 keV wide-band spectra

can be modeled well by a three component partial covering warm absorber model consisting of a dens, a thin and an open region. The ionization parameters ξ of the dens and the thin components are ~ 0.3 and ~ 12 erg cm s^{-1}, respectively. The $N_{\rm H}$ values are ~ 20 and $\sim 1.5 \times 10^{22}$ cm^{-2}, respectively. If we assume that the absorber is located at the outer-edge of the disk, the 200 sec typical dip time scale is converted into the absorber blob geometrical width of $W = 5 \times 10^9$ cm, and the obtained ξ and $N_{\rm H}$ gives absorber blob geometrical thickness of $D = 1$–2×10^8 cm.

Based on these results, we propose an absorber made of dens and thin filaments with a typical size of D in group forming blobs of typical size of W are distributed around the line-of-sight to us, and the blobs' motion and piling-up generates the dips with variety of deepness. In near future, high-sensitivity wide-band observation with high-resolution spectroscopy provided by ASTRO-H will give us a better chance to dig into the physical state of the absorber in much detail.

References

Crosa, L., Boynton P.E. 1980, ApJ, 235, 999
Enoto, T. et al. 2008, PASJ, 60, S57
Giacconi, R., Gursky, H., et al. 1973, ApJ, 184, 227
Leahy, D.A. 1997, MNRAS, 287, 622
Mihara, T., et al. 1991, PASJ, 43, 501
Mitsuda K. et al. 2007, PASJ, 59, 1
Oosterbroek, T. et al. 1997, A&A 327, 215
Reynolds, A.P., Parmar, A.N. 1995, A&A, 297, 747
Shakura, N.J. et al. 1998, MNRAS, 300, 992
Stelzer. B. et al. 1999, A&A, 342, 736
Tananbaum, H., Gursky, H., et al. 1972, ApJ, 174, L143
Terada, Y. et al. 2008, PASJ, 60, S25
Ushimaru, N., Tawara, Y., Koyama, K. 1989, PASJ, 41, 441